Site-specific magnetism of half-metallic Mn_2Ru_xGa thin films determined by x-ray absorption spectroscopy

Davide Betto,[1] Naganivetha Thiyagarajah,[1] Yong-Chang Lau,[1] Cinthia Piamonteze,[2] Marie-Anne Arrio,[3] Plamen Stamenov,[1] J. M. D. Coey,[1] and Karsten Rode[1,*]

[1]*CRANN, AMBER and School of Physics, Trinity College Dublin, Dublin 2, Ireland*

[2]*Swiss Light Source, Paul Scherrer Institute, CH-5232 Villigen PSI, Switzerland*

[3]*IMPMC, F-75015 Paris, France*

(Received 3 December 2014; revised manuscript received 23 February 2015; published 12 March 2015)

The site-specific magnetic properties of thin films of the Heusler compound Mn_2Ru_xGa, $0.6 < x < 1.0$, are studied using x-ray absorption and dichroism spectroscopy. There is evidence of half metallicity up to $x = 0.7$, and compensation of the Mn $4a$ and $4c$ moments in this range, leading to a zero-moment half metal. We also also discuss the effect of substrate-induced strain on the magnetic properties. By tuning the biaxial strain, simultaneous perfect magnetic compensation and half-metallic character is achievable at, below, or above room temperature.

DOI: 10.1103/PhysRevB.91.094410 PACS number(s): 75.50.Gg, 71.20.Be, 61.05.cj, 75.25.−j

I. INTRODUCTION

Both full and half-Heusler alloys are attracting considerable interest due to the remarkable versatility of this family of compounds. They can be metallic, semiconducting, or insulating, and there are members that are ferromagnetic, antiferromagnetic, ferrimagnetic, or nonmagnetic [1–3]. More exotic transport behavior such as a topologically insulating phase has also been observed [4,5].

The recent discovery of a very attractive combination of magnetic and transport properties in a homogeneous Heusler material—high spin polarization, half metallicity, and zero net moment—in thin films of the ferrimagnetic, $C1_b$-ordered, Mn_2Ru_xGa alloy [6] (MRG) suggest that a long-standing gap has been filled. Zero-moment half metals were predicted by van Leuken and de Groot [7], but previous attempts to produce an example of the class had failed. This new type of material may be of considerable technological interest, as it is inherently insensitive to stray fields and free from demagnetizing forces and radiative damping losses, while preserving useful spin-transport functionality. MRG potentially removes some of the obstacles to the integration of magnetic elements in electronic circuits scaled to nanometric dimensions.

In the $C1_b$ structure, Mn occupies two inequivalent crystallographic positions, $4a$ (0,0,0) and $4c$ (3/4,3/4,3/4), while Ga occupies the $4b$ (1/2,1/2,1/2) and Ru some of the $4d$ (1/4,1/4,1/4) positions, respectively. In a simple band picture, the addition of a Ru atom provides both states (twelve) and electrons (eight) to the system. In this model, based on empirical Slater-Pauling rules, the addition of twelve electronic states and eight electrons by one Ru atom per formula should change the magnetization from $-1\mu_B$ f.u.$^{-1}$ to $+1\mu_B$ f.u.$^{-1}$, hence giving perfect compensation at $x = 0.5$, or $Mn_2Ru_{0.5}Ga$. The reality will be less simple. The addition of Ru is likely to change both the shape and the positions of the Mn bands, and the details of the charge transfer to the Ga ligands play an important role in determining the magnetic properties.

*Corresponding author: rodek@tcd.ie

II. EXPERIMENTAL TECHNIQUES

A series of Mn_2Ru_xGa samples was produced on MgO (100) substrates by magnetron cosputtering from a Mn_2Ga and a Ru target. The stoichiometry of the samples was controlled by the power supplied to each of the guns. Immediately after deposition, the samples were covered with a ∼2 nm Al_2O_3 layer to prevent oxidation. More details about the growth procedure are provided elsewhere [6].

X-ray diffraction data were recorded on all samples, including x-ray reflectivity, 2θ-θ scans, and reciprocal space maps (RSMs), to determine in-plane and out-of-plane lattice parameters and grain size, film thickness, roughness, and density.

In order to rapidly determine the Ru concentration x, we deposited a pure Ru thin film using the deposition conditions of the MRG samples, as well as four MRG samples with varying power to the Mn_2Ga sputtering target. From the measured x-ray density and the lattice parameters of these five samples, the relation between the x-ray density and the Ru concentration x could be established.

X-ray absorption spectroscopy (XAS) spectra on the Mn $L_{3,2}$ edges were recorded in an applied magnetic field of $\mu_0 H = 6.8$ T with the sample normal parallel to both the x-ray propagation vector $\vec{k}$ and the applied magnetic field. The sample temperature was varied from 2 to 360 K [8]. We also recorded XAS spectra on the Ga $L_{3,2}$ and the Ru $M_{3,2}$ edges. We found no absorption edge in the energy range corresponding to Ga, indicating that it is close to a $3d^{10}$ configuration. The signal-to-noise ratio on the Ru edges was too poor to extract any magnetic or structural information.

L-edge x-ray absorption and dichroism allow the independent determination of the spin $2\langle S_z\rangle$ and orbital $\langle L_z\rangle$ moments via the magneto-optical sum rules [9]. It is chemically selective due to the separation of the atomic absorption edges in energy, and specific sites can be identified due to the effect of the crystal field on the multiplet structure. The case of Mn is complicated by two main factors. First, the $2p$ spin-orbit coupling is insufficient to clearly separate the L_3 ($^2P_{3/2}$) from the L_2 ($^2P_{1/2}$) edge, and, second, there is a significant degree of L_2 character in the L_3 absorption peak and vice versa.

The common way to circumvent this problem is to assume that the values for the magnetic moments obtained by the sum rules have to be multiplied by a factor ∼1.5 in the case of Mn [10], to obtain agreement with other magnetometry methods. We address this differently. For a direct comparison with an explicit quantum mechanical core-hole corrected multiplet calculation, we use the code initially written by Cowan, and further developed by Thole [11], and calculate the theoretical absorption and dichroism spectra for the two Mn crystallographic positions. The magnetic moments are then given by the calculated expectation values of $\langle S_z \rangle$ and $\langle L_z \rangle$. The experimentally observed magnetic moments are subsequently obtained by scaling the calculated dichroic signal to the observed x-ray magnetic circular dichroism (XMCD).

In intermetallic systems, we expect a high degree of charge transfer between the different ions in the unit cell. It has, however, been reported that Mn in these alloys retains a partially localized electronic configuration [12,13]. We therefore based our calculated spectra on a model where Mn is in a $3d^5$ ground configuration with charge transfer by interaction with a $3d^6\underline{L}$ configuration, where $\underline{L}$ denotes a ligand hole. We used literature values for the transfer integrals $T_{t_{2g}} = 0.9$ eV and $T_{e_g} = 2.0$ eV. The difference between the U_{dd} and U_{pd} Hubbard potentials was chosen to be 1.12 eV [14]. In the Heusler structure, Mn occupies one site that is octahedrally coordinated by Ga and another that is tetrahedrally coordinated, as discussed above. We used 1.2 and 0.5 eV for the respective crystal field parameters $10Dq$. The Slater integrals were reduced to 80% of their atomic values. The charge-transfer parameters Δ were set to the values that best reproduce the experimental data: 4.0 and −4.0 eV for the $4c$ and $4a$ positions, respectively. They are the only free parameters in our model. The remarkably large difference in charge transfer from the ligands to the Mn of opposite spins in the two different positions indicates the degree of charge delocalization needed to displace sufficiently the states close to the Fermi level, thereby producing high spin polarization while retaining net moment compensation.

In Fig. 1 we show the experimental data along with the calculated contribution from the two, antiferromagnetically coupled, sites. We also identify a small (5%) contribution from Mn^{3+}, which is likely to be an oxide in the grain boundaries in the film. An estimate of the grain surface-to-volume ratio can be obtained from the average grain size as measured by RSM. We find that the in-plane coherence length is ∼150 nm, implying that ∼2.6% of the Mn is present in these boundaries, assuming the boundary is one atomic layer thick. We calculated this contribution as a Mn^{3+} ion with $10Dq = 0.5$ eV. The calculated and experimental spectra show excellent agreement with each other. We find zero-temperature expectation values $2\langle S_z \rangle$ of $4.35\mu_B$ and $4.85\mu_B$ with $3d$ occupation numbers of 5.65 and 5.15 for the $4a$ and $4c$ positions, respectively. The orbital moment $\langle L_z \rangle$ and the dipolar moment $\langle T_z \rangle$ are found to be ∼0 for both positions, as expected for Mn in the $3d^5$ configuration. In view of recent neutron diffraction measurements [13] and density functional theory (DFT) calculations [15] of Mn moments of related compounds, the value of $2\langle S_z \rangle$ obtained from the fits and the multiplet approximation are likely to be about 30% too high.

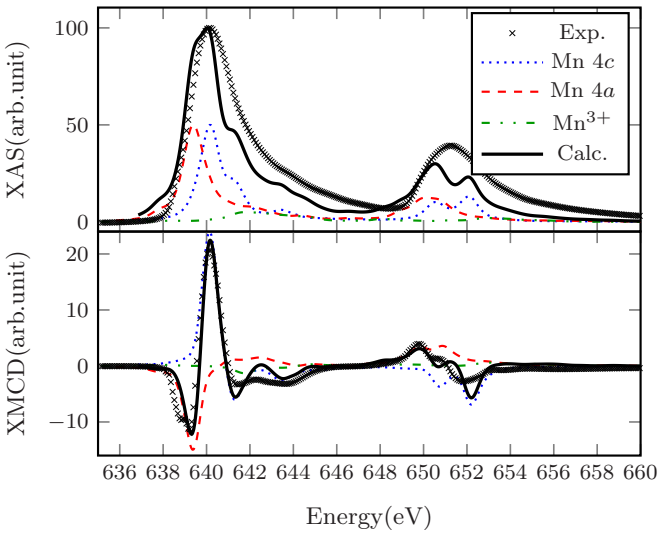

FIG. 1. (Color online) The isotropic x-ray absorption and dichroism spectra for a typical Mn_2Ru_xGa sample. The calculated contribution from each crystallographic position is shown in thin dotted/dashed lines. The dichroic spectra for each site has opposite sign for the two positions $4a$ and $4c$, confirming their antiferromagnetic ordering.

III. RESULTS AND DISCUSSION

In Fig. 2 we show the temperature dependence of the spin moments for a typical sample. There is a clear variation of the magnitudes of the moments of MRG samples with different Ru levels and c/a ratios, however, the general trend

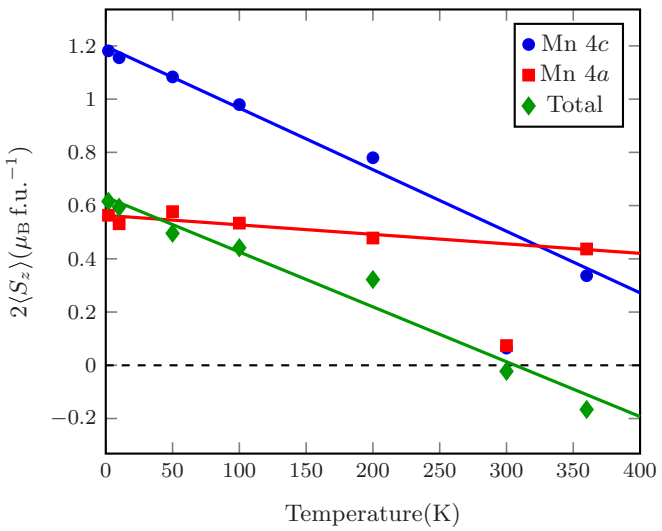

FIG. 2. (Color online) Temperature dependence of the magnetization (absolute values) of a selected sample, with $x = 0.98$. The change of sign of the magnetization occurs at $T_{comp} \sim 310$ K, in good agreement with the compensation temperature measured by the spontaneous Hall effect. The lines are guides to the eye only. At $T = 300$ K, the sample is almost perfectly compensated, and we were unable to achieve even partial magnetic saturation with the maximum applied field available ($\mu_0 H = 6.8$ T), hence the deduced spin moments tend towards 0.

is the same for all samples. The 4c magnetization decreases linearly with temperature and reaches zero at an extrapolated temperature $T_C\,(4c) \sim 550$ K, in good agreement with the behavior reported for bulk powders of Mn_2RuGa [16]. The 4a magnetization remains almost constant over the temperature range measured. Due to this difference in temperature dependence, the sign of the magnetization changes at a temperature that depends on both Ru concentration x and on the degree of substrate-induced strain.

The observed site moments and saturation magnetization are much lower than the calculated expectation values, or the values determined by neutron diffraction in tetragonal Mn_3Ga [13]. There are several reasons for this. First, the XAS/XMCD was recorded in an applied magnetic field of $\mu_0 H = 6.8$ T, insufficient to completely magnetize the samples at all experimental temperatures, especially close to compensation, where the anisotropy field becomes very large. The nature of the magnetic domains in a zero-moment material is not yet well understood. We speculate that domains are present as they are in antiferromagnets, and that the domain structure is not easily eliminated in an applied field. Second, the relatively small grain sizes (~150 nm) suggest that there may be a large number of antiphase boundaries present in the samples. These are likely to couple antiferromagnetically, and hence reduce the magnetization observed by XMCD. Third, we cannot completely exclude the possibility of a small fraction of antisites [Mn (4a) occupying the 4b Ga position]. The two sites are equivalent by symmetry, and if they coupled antiferromagnetically, the XMCD of the pair would be zero.

In order to investigate the effect of the changing Ru concentration and the strain, we have chosen to extrapolate the magnetic properties to $T = 0$ K by linear regression. This extrapolation has no particular physical significance, but, as mentioned above, the linear trend in temperature is observed for all the samples measured and hence provides a good indication of their behavior at 0 K.

In Fig. 3 we trace the evolution of the absolute value of the spin moment of the 4a and 4c positions as a function of the Ru concentration x. The 4a magnetization remains mostly unchanged with increasing x, indicating that the Fermi level does not cross the band edges originating primarily from the corresponding reciprocal lattice position. The large spread of the values around the inferred spin moment $2\langle S_z\rangle\,(4a) = 0.68\mu_B$ is due to the varying c/a ratio, discussed below.

The 4c position, on the contrary, exhibits a sharp increase in magnetization between 0.60 and 0.75. The zero-temperature sign of the total magnetization changes near $x = 0.65$. This sharp increase is followed by a change of slope for $x > 0.75$, the 4c magnetization increasing moderately for $0.7 < x < 1.2$. We interpret this as follows. Hybridization of bands originating from the Mn in the 4c position with those of Ru in 4d has two effects: it reduces the Mn 4c spin splitting and simultaneously it pulls the minority spin band down towards the Fermi level, thus changing the magnetization of this crystallographic position. The rate of change depends on the details of the band structure, leading to an abrupt change in the 4c spin-up occupied density of states at $x \sim 0.7$.

We now turn to the effect of substrate-induced strain. The variation of the magnetization in MRG is dominated by the change in Ru concentration, as can be seen in Fig. 3.

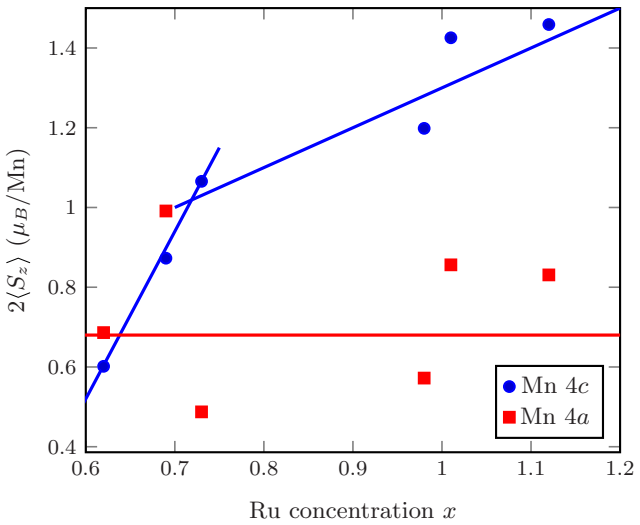

FIG. 3. (Color online) Evolution of the absolute value of the magnetic moments at of the two Mn positions, extrapolated to $T = 0$ K, with Ru concentration x. The solid lines are linear regressions to the data sets. In the case of Mn 4c, we identify a change of slope in the vicinity of $x = 0.7$, corresponding to the onset of filling the minority spin channel of Mn in this position.

The addition of Ru adds both electrons and states to the system as discussed above, but also provides chemical pressure, effectively modifying the strain, as observed by the change in c/a ratio. This ratio can furthermore be controlled by choosing an appropriate substrate, *or* by tuning the film thickness. In this set of experiments we have used the latter option. In order to quantify the effect of strain, we therefore infer the magnetization of a virtual sample with $x = 1.0$ for each experimental c/a ratio, following the variation shown in Fig. 3.

In Fig. 4 we plot the variation of the site-specific magnetization as a function of the c/a ratio determined by RSM. The 4c magnetization is decreasing with increasing c/a ratio, indicating that the compressive strain provided by the MgO substrate [$\sqrt{2}a_0\,(\mathrm{MgO}) = 5.956$ Å] gradually empties the 4c band by increasing its position in energy. Conversely, in the region of moderate strain ($c/a \sim 1.8\%$–2.0%), the 4a magnetization increases. Above $c/a \sim 2.0\%$, the 4a bands deform sufficiently, changing their curvature close to the Fermi level, and a greater number of delocalized (conduction electron) states becomes available, resulting in a net decrease in the localized magnetic moment.

The calculation of the dichroic spectra using the multiplet code allows a reasonably accurate determination of the site-specific magnetic properties of Mn_2Ru_xGa, as can be seen from the excellent agreement between the calculated and the experimental spectra. The parameters in our model are largely based on accepted values for Mn, but a more precise analysis would require a more accurate determination of the same. XAS is by nature rather insensitive to subtle variations in charge transfer between ligands due to the screening of the core hole by the 3d electrons. X-ray photoelectron spectroscopy (XPS) and ultraviolet photoelectron spectroscopy (UPS) do not suffer from this limitation, and would provide a means to determine the charge-transfer parameters more accurately.

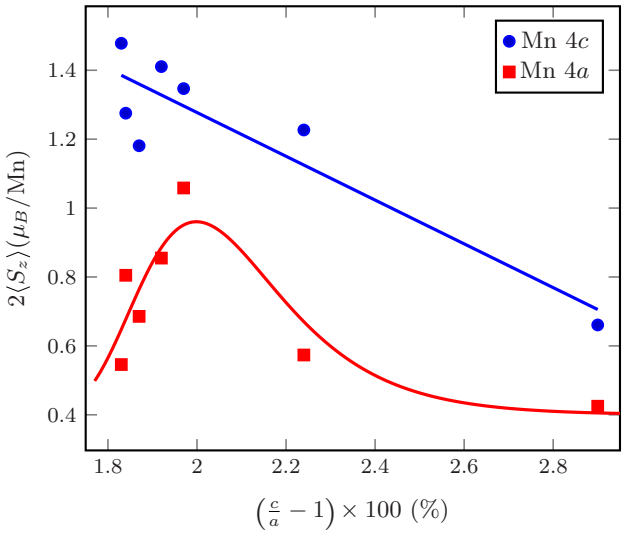

FIG. 4. (Color online) Site-specific magnetization (absolute values) extrapolated to $T = 0$ K as a function of the c/a ratio for the samples with their spin moments translated to a virtual $x = 1.0$ Ru concentration, as discussed in the text. The solid lines are guides to the eye only.

IV. CONCLUSION

Previously, we have demonstrated that Mn_2Ru_xGa exhibits a high spontaneous Hall angle (ρ_{xy}/ρ_{xx}), which is abruptly changing sign for a small variation in x. This is coupled with a high Fermi-level spin polarization, measured by point contact Andreev reflection (PCAR) spectroscopy, indicating that the spin polarization of Mn_2Ru_xGa is in excess of 55% [6]. While this is well short of the 100% expected for a half metal, it is in the same range reported for other established Heusler half metals. Spin-polarized photoemission may provide a better measure of spin polarization in a wider energy range close to the Fermi energy.

Here we have demonstrated that the electronic structure as observed by XAS/XMCD is compatible with a half-metallic state in Mn_2Ru_xGa when $x < 0.7$, but due to the inherent difficulty of saturating the samples, we underestimate the change in spin moment with increasing Ru content x. The nonmonotonic behavior of the spin moment as a function of lattice strain is a signature of a complex band structure, indicating that the rigid band, Slater-Pauling-like analysis of the magnetic properties is inadequate for MRG. We have shown that the electronic structure of Mn_2Ru_xGa is tunable both by changing the Ru concentration x and by straining the epitaxial thin film. In order to retain high spin polarization, the Ru concentration needs to stay below $x = 0.7$. In this regime, a moderate strain of $c/a \sim 2\%$ ensures that complete magnetic compensation can be achieved in the near room temperature, thus opening prospects of using this class of materials in spin electronic devices. Research into the nature of the magnetic domains and micromagnetic structure at small physical dimensions, the details in the behavior of the order parameter, spin injection and diffusion, as well as millimeter-wave magnetic resonance and damping losses in this or related alloys should provide captivating fundamental knowledge on the nature of the compensated ferrimagnetic state and suggest opportunities for its practical use.

ACKNOWLEDGMENTS

This work was supported by Science Foundation Ireland through AMBER, and from Grant No. 13/ERC/I2561. K.R. acknowledges financial support from the European Community's Seventh Framework Programme IFOX, NMP3-LA-2010-246102. D.B. acknowledges financial support from IRCSET. The x-ray absorption measurements were performed on the EPFL/PSI X-Treme beamline at the Swiss Light Source, Paul Scherrer Institut, Villigen, Switzerland. The research leading to these results has received funding from the European Community's Seventh Framework Programme (FP7/2007-2013) under Grant Agreement No. 312284(CALIPSO). The authors would like to thank H. Kurt, M. Žic, and T. Archer for fruitful discussions.

[1] T. Graf, J. Winterlik, L. Müchler, G. H. Fecher, C. Felser, and S. S. P. Parkin, Magnetic Heusler compounds, in *Handbook of Magnetic Materials* (Elsevier, Amsterdam, 2013), Chap. 1, pp. 1–75.

[2] B. Balke, G. Fecher, and C. Felser, New Heusler compounds and their properties, in *Spintronics*, edited by C. Felser and G. H. Fecher (Springer, Berlin, 2013), pp. 15–43.

[3] M. Hakimi, M. Venkatesan, K. Rode, K. Ackland, and J. M. D. Coey, The zero-magnetization Heusler ferrimagnet, J. Appl. Phys. **113**, 17B101 (2013).

[4] S. Chadov, X. Qi, J. Kübler, G. H. Fecher, C. Felser, and S. C. Zhang, Tunable multifunctional topological insulators in ternary Heusler compounds, Nat. Mater. **9**, 541 (2010).

[5] H. Lin, L. A. Wray, Y. Xia, S. Xu, S. Jia, R. J. Cava, A. Bansil, and M. Z. Hasan, Half-Heusler ternary compounds as new multifunctional experimental platforms for topological quantum phenomena, Nat. Mater. **9**, 546 (2010).

[6] H. Kurt, K. Rode, P. Stamenov, M. Venkatesan, Y.-C. Lau, E. Fonda, and J. M. D. Coey, Cubic Mn_2Ga thin films: Crossing the spin gap with ruthenium, Phys. Rev. Lett. **112**, 027201 (2014).

[7] H. van Leuken and R. A. de Groot, Half-metallic antiferromagnets, Phys. Rev. Lett. **74**, 1171 (1995); R. A. de Groot, F. M. Mueller, P. G. van Engen, and K. H. J. Buschow, New class of materials: Half-metallic ferromagnets, *ibid.* **50**, 2024 (1983).

[8] C. Piamonteze, U. Flechsig, S. Rusponi, J. Dreiser, J. Heidler, M. Schmidt, R. Wetter, M. Calvi, T. Schmidt, H. Pruchova, J. Krempasky, C. Quitmann, H. Brune, and F. Nolting, X-Treme beamline at SLS: X-ray magnetic circular and linear dichroism at high field and low temperature, J. Synchrotron Radiat. **19**, 661 (2012).

[9] P. Carra, B. T. Thole, M. Altarelli, and X. Wang, X-ray circular dichroism and local magnetic fields, Phys. Rev. Lett. **70**, 694 (1993).

[10] H. A. Dürr, G. van der Laan, D. Spanke, F. U. Hillebrecht, and N. B. Brookes, Electron-correlation-induced magnetic order of ultrathin Mn films, Phys. Rev. B **56**, 8156 (1997).

[11] R. D. Cowan, *Theory of Atomic Structure and Spectra*, Los Alamos Series in Basic and Applied Sciences (University of California Press, Berkeley, CA, 1981); B. Thole, G. van der Laan, and P. H. Butler, Spin-mixed ground state of Fe phthalocyanine and the temperature-dependent branching ratio in x-ray absorption spectroscopy, Chem. Phys. Lett. **149**, 295 (1988).

[12] M. Meinert, J.-M. Schmalhorst, C. Klewe, G. Reiss, E. Arenholz, T. Böhnert, and K. Nielsch, Itinerant and localized magnetic moments in ferrimagnetic Mn_2CoGa thin films probed by x-ray magnetic linear dichroism: Experiment and *ab initio* theory, Phys. Rev. B **84**, 132405 (2011).

[13] K. Rode, N. Baadji, D. Betto, Y.-C. Lau, H. Kurt, M. Venkatesan, P. Stamenov, S. Sanvito, J. M. D. Coey, E. Fonda, E. Otero, F. Choueikani, P. Ohresser, F. Porcher, and G. André, Site-specific order and magnetism in tetragonal Mn_3Ga thin films, Phys. Rev. B **87**, 184429 (2013).

[14] M. Taguchi, P. Krüger, J. C. Parlebas, and A. Kotani, Theoretical study of resonant x-ray emission spectroscopy of Mn films on Ag, Phys. Rev. B **73**, 125404 (2006).

[15] L. Wollmann, S. Chadov, J. Kübler, and C. Felser, Magnetism in cubic manganese-rich Heusler compounds, Phys. Rev. B **90**, 214420 (2014).

[16] T. Hori, M. Akimitsu, H. Miki, K. Ohoyoama, and Y. Yamaguchi, Magnetic properties of $(Mn_{1-x}Ru_x)_3Ga$ alloys, Appl. Phys. A **74**, s737 (2002).